

# Biomimetic Synthesis of Natural and “Unnatural” Lignans by Oxidative Coupling of Caffeic Esters

Carmelo Daquino,<sup>[a]</sup> Antonio Rescifina,<sup>[a]</sup> Carmela Spatafora,<sup>[a]</sup> and Corrado Tringali\*<sup>[a]</sup>

**Keywords:** Oxidation / Lignans / Biomimetic synthesis / Reaction mechanisms / Manganese

The metal-mediated oxidative coupling of caffeic acid esters has been employed in the biomimetic synthesis of dimeric lignans and neolignans. Phenethyl and methyl caffeate esters were used as substrates and MnO<sub>2</sub>, Mn(OAc)<sub>3</sub> and Ag<sub>2</sub>O as oxidative coupling agents. The manganese-mediated reactions afforded in good yields the unusual benzo[*kl*]xanthene lignans **6** and **15** as the major products accompanied by minor amounts of the arylidihydronaphthalene lignans

(±)-**7** and (±)-**16**. When Ag<sub>2</sub>O was employed, the neolignan (±)-**17** was obtained as the major product. This biomimetic route was also used to obtain the natural benzo[*kl*]xanthene lignans rufescidride (**9**) and mongolicumin A (**10**). A computational study of the coupling reactions was also carried out.

(© Wiley-VCH Verlag GmbH & Co. KGaA, 69451 Weinheim, Germany, 2009)

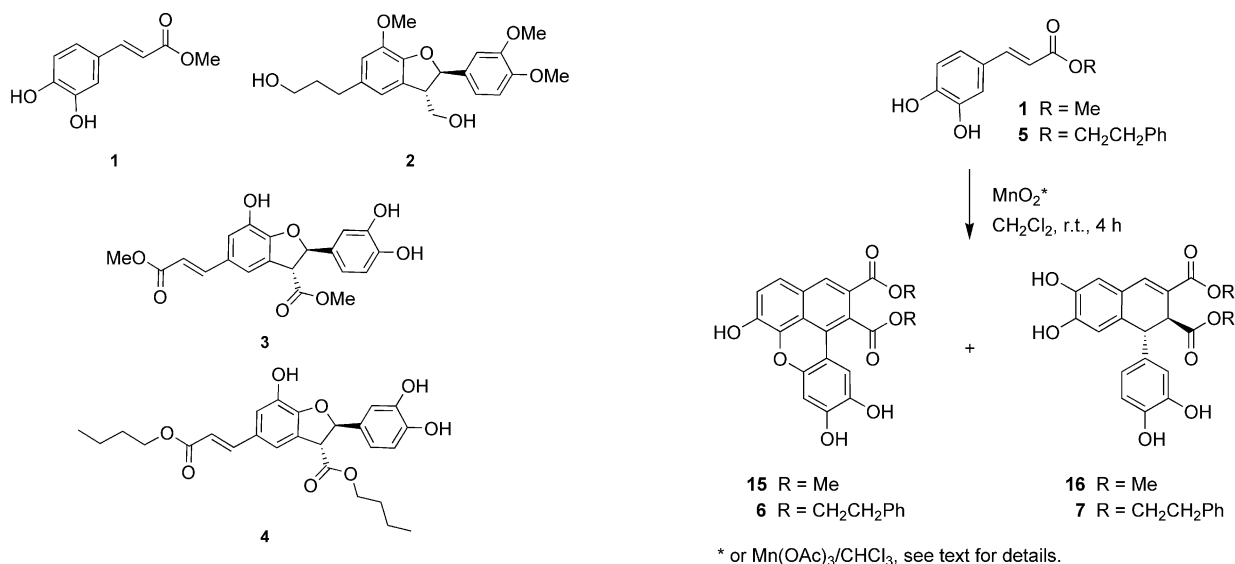
## Introduction

Lignans and related compounds (neolignans, oxyneolignans and mixed lignans) are widely distributed within the plant kingdom. In these plant secondary metabolites carbon skeletons are normally formed of two phenylpropanoid (C<sub>6</sub>C<sub>3</sub>) units. Notwithstanding this relatively simple basic skeleton, their structural diversity is really remarkable. Their biosynthetic origin is the shikimate pathway: the term “lignan”, originally introduced by Haworth<sup>[1]</sup> and related to the woody tissue from which many of the first specimens were obtained, refers to dimers generated by β–β′ (8–8′) oxidative coupling of two cinnamic acid residues. According to IUPAC recommendations,<sup>[2]</sup> “neolignans” are dimers that originate from coupling other than 8–8′ coupling, although the term “lignan” is frequently employed in a broader sense (including neolignan), as in the title of this article. Lignans, neolignans and other related compounds are accumulated in vascular plants as a chemical defence system,<sup>[3]</sup> and this may explain their diverse biological activities, including cytotoxic,<sup>[4]</sup> antimitotic, antileishmanial,<sup>[5]</sup> antiangiogenic,<sup>[6]</sup> cardiovascular<sup>[7]</sup> and antiviral activity.<sup>[8]</sup> The biological activities and structural variety of lignans and related compounds make them an attractive target for chemical synthesis or modification. In particular, biomimetic coupling reactions carried out on natural precursors may afford “unnatural” products through a radical phenolic oxidative coupling mechanism that mimic the

“natural” biosynthetic process. Thus, it is possible, in principle, to obtain compounds unprecedented in the literature that maintain a basic “natural” skeleton and possibly offer a bioactivity profile similar to, or better than, that of a natural analogue. Owing to the lack of stereocontrol both in metal- or enzyme-mediated phenolic radical coupling reactions, racemic mixtures are frequently obtained.<sup>[9]</sup> Nevertheless, a number of interesting products have been obtained in such a way and in some cases the bioactive racemate has been resolved to obtain the most active enantiomer. In this regard, one interesting example is the reported dimerization of methyl caffeate (**1**) with Ag<sub>2</sub>O,<sup>[10]</sup> which affords a neolignan racemate related to the natural dimer 3′,4-di-*O*-methylcedrusin (**2**). This latter was isolated as one of the active compounds in “dragon’s blood”, the blood-red latex produced by some *Croton* spp. growing in South America and employed in traditional medicine for its wound-healing and anticancer properties. The racemate was then resolved to give the (2*R*,3*R*) enantiomer (**3**), which shows promising antitumour properties against breast cancer cell lines and is more potent than its (2*S*,3*S*) enantiomer, not only as an antiproliferative but also as an antiangiogenic agent.<sup>[5]</sup> In addition, the related neolignan racemate (±)-**4** [only the (2*R*,3*R*) enantiomer is reported] has been found to be highly active against chloroquine-resistant *Plasmodium falciparum* and *Leishmania donovani*.<sup>[4a]</sup>

The interesting biological properties of these natural and synthetic neolignans, together with the increasing attention devoted to antiangiogenic agents in cancer therapy,<sup>[11a,11b]</sup> prompted us to carry out a biomimetic synthesis of new “unnatural” neolignans as a continuation of our search for bioactive analogues of natural products.<sup>[12]</sup> The results of this work are reported below.

[a] Dipartimento di Scienze Chimiche, Università degli Studi di Catania, Viale A. Doria 6, 95125 Catania, Italy  
Fax: +39-095-580138  
E-mail: ctringali@unict.it

Scheme 1. Oxidative coupling of compounds **1** and **5**.

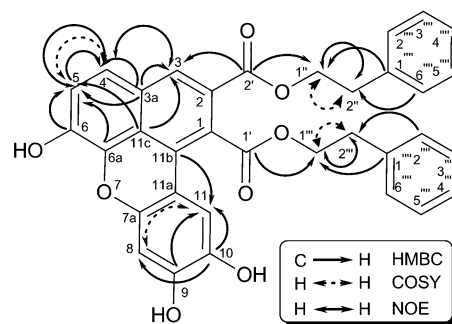
## Results and Discussion

First, we selected CAPE (caffeic acid phenethyl ester, **5**) as the substrate for the oxidative coupling reaction. This natural product is a component of propolis and it is reported to be an anti-inflammatory, antioxidant and antitumour agent.<sup>[13a–13d]</sup> To the best of our knowledge, CAPE had never been employed previously in phenolic oxidative coupling reactions, so we expected unreported dimerization products from this biomimetic coupling process. The reaction was carried out initially on an analytical scale at room temperature, employing  $\text{MnO}_2$  in dichloromethane as the oxidative agent (Scheme 1). After 1 h, monitoring of the reaction mixture by HPLC–UV showed the presence of two main products **6** and **7**, together with a large amount of unreacted **5**. By prolonging the reaction time up to 4 hours, a higher product/substrate ratio was observed. Preparative coupling afforded a green crude reaction mixture. To avoid further oxidation of the products, the reaction was quenched by the careful addition of ascorbic acid. After DIOL silica gel purification two products, **6** (48%) and **7** (16.5%), were obtained, together with residual **5**.

Compound **6** showed a negative ESI-MS peak at  $m/z = 561$  ( $[\text{M} - \text{H}]^-$ ), which suggested the formation of a tetrahydro dimer of **5**. This was confirmed by elemental analysis, which established the molecular formula  $\text{C}_{34}\text{H}_{26}\text{O}_8$ , lacking four hydrogen atoms with respect to a simple dimerization product. The  $^1\text{H}$  and  $^{13}\text{C}$  NMR spectroscopic data for **6** are reported in the Exp. Sect.; these data appeared immediately not to be consistent with those of the most frequently reported caffeic dimers, such as the dihydrobenzofuran neolignans **3** and **4**.<sup>[14]</sup>

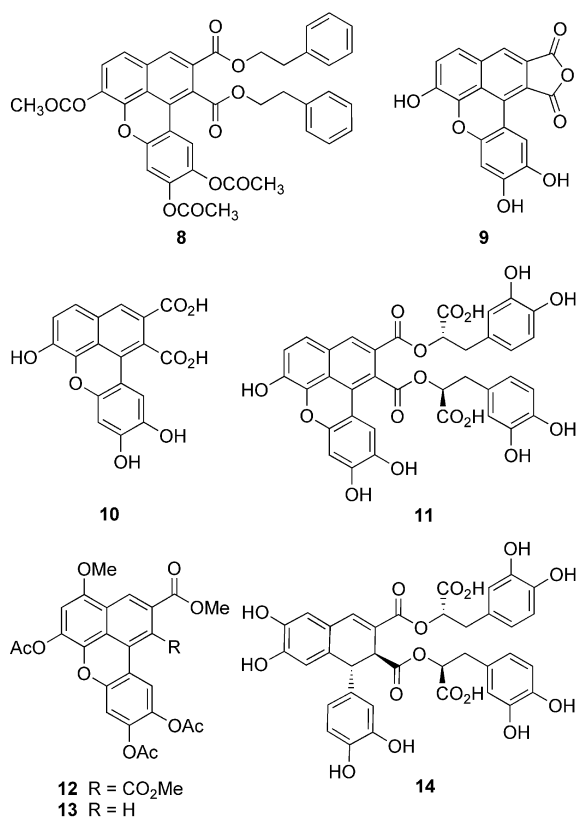
Both spectra showed some signals attributable to two non-equivalent phenethyl moieties. In addition, further low-field signals were observed in the  $^1\text{H}$  NMR spectrum indicating a significant modification of the caffeic acid substructures. The  $^{13}\text{C}$  NMR spectroscopic data suggested that two degrees of unsaturation could reasonably be attributed

to new cycles. The UV spectrum of **6** [ $\lambda_{\text{max}} = 386 \text{ nm}$  ( $\epsilon = 11000 \text{ M}^{-1} \text{ cm}^{-1}$ )] was indicative of an extensively conjugated system and the product exhibited intense fluorescence under UV light (366 nm) with emission at  $\lambda_{\text{max}} = 513 \text{ nm}$  and  $\Phi_{\text{F}} = 0.7$  (referenced to anthracene). The IR spectrum showed, as expected, intense absorption bands for the hydroxy and conjugated ester groups ( $\tilde{\nu}_{\text{max}} = 3532$  and  $1716 \text{ cm}^{-1}$ , respectively). Acetylation of **6** afforded a peracetate **8**, clearly demonstrated by the presence of three acetoxy groups in the ESI-MS and  $^1\text{H}$  NMR spectra, which indicates that three acetylatable hydroxy groups are present in the structure of **6**. Further data were obtained by NMR experiments, namely NOE, HSQC and HMBC data (Figure 1).

Figure 1. Selected COSY, NOE and HMBC correlations for compound **6**.

On the basis of these data, a careful literature search allowed us to identify the conjugated nucleus of the dimer **6** as a benzo[*k*]xanthene structure. In fact, the  $^1\text{H}$  and  $^{13}\text{C}$  NMR spectroscopic data of the natural benzoxanthene lignans rufescidride (**9**), mongolicumin A (**10**) and yunnaneic acid H (**11**), isolated, respectively, from *Cordia rufescens*,<sup>[15]</sup> *Taraxacum mongolicum*<sup>[16]</sup> and *Salvia yunnanensis*,<sup>[17]</sup> almost superimpose those of the dimer **6**, the structure of which was consequently established. Benzo[*k*]xanthene lig-

nans are rarely reported either as natural products or products of oxidative coupling. Maeda et al. obtained benzo[*kl*]-xanthenes such as **12** and **13**<sup>[18]</sup> in low yields by employing caffeic acid derivatives as substrates and Ag<sub>2</sub>O as the oxidative agent followed by acetylation of the dimeric product. The NMR spectroscopic data of the core structures of these benzoxanthenes are also in perfect agreement with those reported herein for compounds **6** and **8**.



The minor product **7** showed a negative ESI-MS peak at  $m/z = 565$  ( $[M - H]^-$ ), which suggests a dehydro dimer of **5**. The molecular formula C<sub>34</sub>H<sub>30</sub>O<sub>8</sub> was determined by elemental analysis. The <sup>1</sup>H and <sup>13</sup>C NMR spectroscopic data of **7** are reported in the Exp. Sect. It was evident that, in addition to the two couples of phenethyl pendants and phenolic rings, two new high-field signals were present [ $\delta = 4.36/46.0$  (<sup>1</sup>H/<sup>13</sup>C) and 3.86/48.3 ppm (<sup>1</sup>H/<sup>13</sup>C)] as part of the four-spin system C-1/C-4 established through a COSY NMR experiment (Figure 2). A literature search rapidly suggested that **7** could have the structure of an aryldihydronaphthalene lignan. This was confirmed by comparison with the data reported for the natural lignan radosiin (**14**) isolated from *Rabdosia japonica*.<sup>[19]</sup> A number of aryldihydronaphthalene lignans have previously been reported in the literature derived either from natural sources<sup>[20]</sup> or as products of the phenolic oxidative coupling of phenylpropanoids.<sup>[21]</sup> A chiral HPLC analysis confirmed that **7** was, as expected, a racemic mixture. The *trans* stereochemistry of the substituents at C-1 and C-2 in ( $\pm$ )-**7** [only the (1*R*,2*S*) enantiomer is reported in Scheme 1] was established on the basis of the  $J_{1,2}$  value (2.5 Hz), corroborated by NOE data and in agreement with  $J$  values reported for other *trans*-

aryldihydronaphthalene lignans.<sup>[9,18,22]</sup> The *trans* stereochemistry is consistent with the diastereoselectivity observed in previously reported syntheses of aryldihydronaphthalene lignans by oxidative coupling in which the main product is normally a *trans* racemic mixture.<sup>[17,18]</sup>

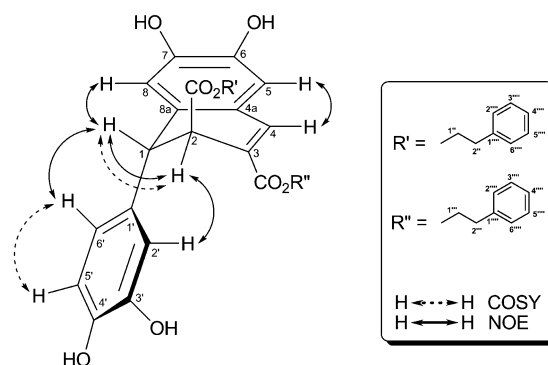


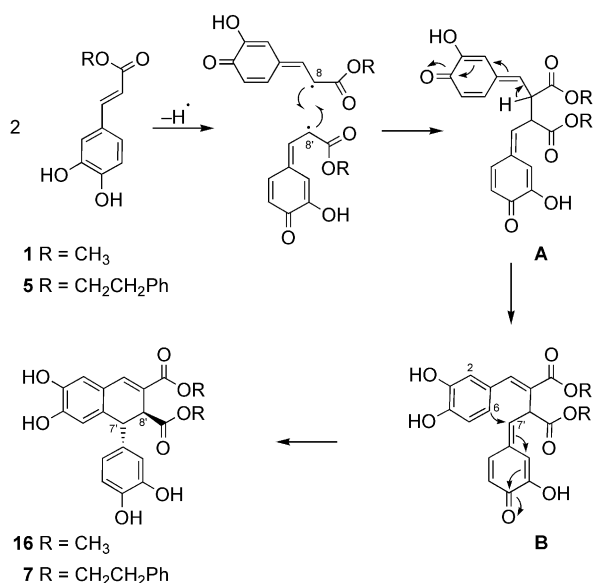
Figure 2. COSY and NOE correlations for compound ( $\pm$ )-**7**.

Once the structures of the products **6** and ( $\pm$ )-**7** had been established, we decided to check the general applicability of this oxidative coupling reaction and at the same time to verify whether the bulk phenethyl pendant could have a role in the formation of the products. Thus, we carried out the reaction under analogous conditions (MnO<sub>2</sub> in CHCl<sub>3</sub> at room temperature) by employing methyl caffeate (**1**) instead of CAPE (**5**) as the substrate. Purification and spectral analysis of the products confirmed the expected formation of the benzo[*kl*]xanthene lignan **15** as the main product (isolated yield 51%) and the dihydronaphthalene lignan ( $\pm$ )-**16** as the minor product (isolated yield 7%; Scheme 1).

At this point we examined in detail the mechanism for the formation of these products. Although the reaction mechanisms previously reported for phenolic oxidative coupling reactions have only rarely been supported by experimental data or calculations, the formation of aryldihydronaphthalene lignan analogues of **7** and **16** has been described and the mechanism is shown in ref.<sup>[16]</sup>, Scheme 2, where only the (1*R*,2*S*) enantiomers are again reported.

In this mechanism, after the formal removal of a hydrogen atom from the *p*-phenolic group of **1** (or **5**), a phenoxy radical with the unpaired electron at the  $\beta$  position may couple with another  $\beta$  radical (8–8' coupling) to generate a reactive bis-quinonemethide **A**. Its tautomer **B** undergoes an intramolecular cyclization (6–7'), that is, an electrophilic aromatic substitution at the 6-position of the activated aromatic ring,<sup>[23]</sup> to give the product ( $\pm$ )-**7** [or ( $\pm$ )-**16**].

The formation of the benzo[*kl*]xanthene lignans **6** and **15** is less obvious. Indeed, only Maeda et al.<sup>[18]</sup> have previously proposed possible mechanisms for the formation of benzoxanthene lignans, but these mechanisms cannot reasonably explain the formation of **6** and **15**. We examined various alternative hypotheses and we came to the conclusion illustrated in Scheme 3, which has been corroborated by the calculations discussed below. In the mechanism proposed by us, both the dimeric products **6/15** and ( $\pm$ )-**7/16** could originate by the same 8–8' coupling reaction, generating the



Scheme 2. Mechanism for the formation of compounds (±)-7 and (±)-16.

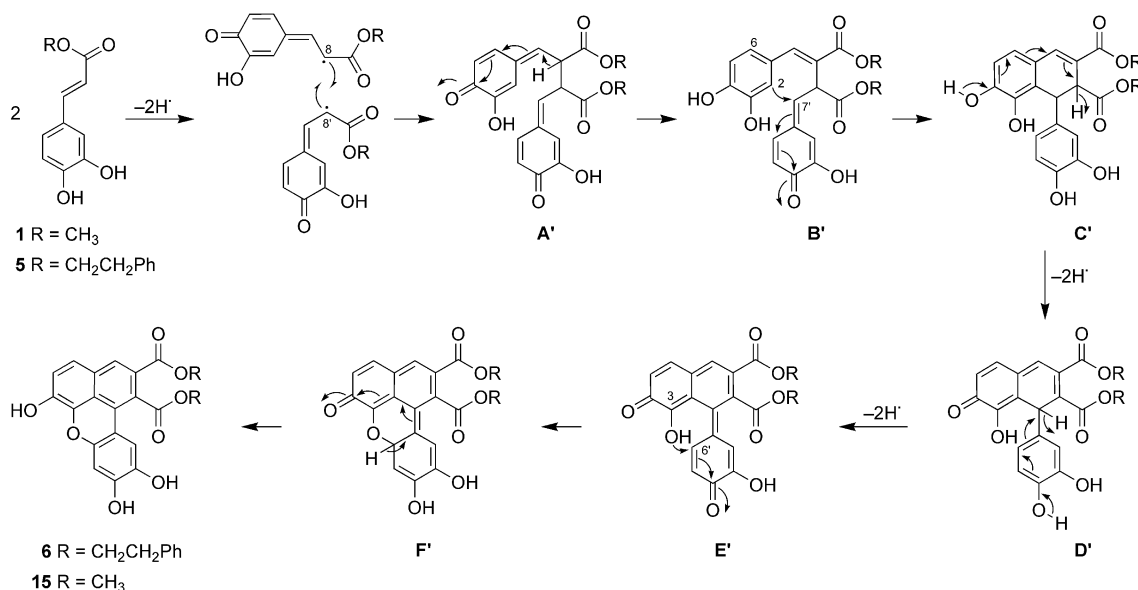
quinonemethide intermediate **A'**. This is followed by a step in which the only difference between the two mechanisms is the position of the hydroxy group *meta* to the propenyl chain, that is, “*exo*” in the formation of **7/16** (intermediate **B**, see Scheme 2), whereas it is “*endo*” (intermediate **B'**) in the formation of **6/15**. Note here that **A** and **A'** are geometrical isomers that could be present in solution together with all the other possible *E/Z* stereoisomers. Intermediates **B** and **B'**, from which the transition states originate, are conformational isomers and may be easily interchanged.

A 2–7' intramolecular cyclization step, very similar to that reported in Scheme 2, gives rise to the aryldihydro-naphthalene intermediate **C'**. Two further oxidative steps on **C'** lead sequentially to the intermediates **D'** and **E'**. Inter-

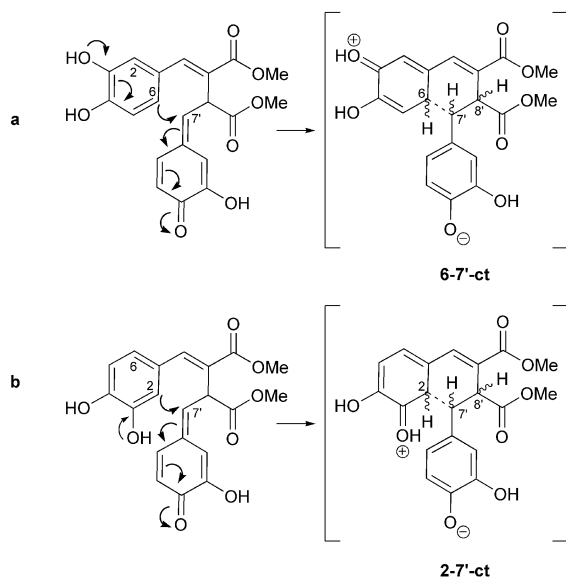
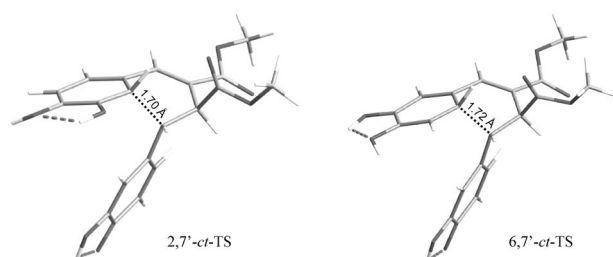
mediate **E'** undergoes further cyclization through nucleophilic attack of the 3-OH on the 5'-position of the quinonemethide moiety, giving rise to the intermediate **F'**, which then tautomerizes into the final products **6/15**. To support this proposed mechanism an *in silico* study at the AM1 level was conducted starting from the intermediates **B** and **B'**. The best results, in terms of activation energy and product ratio, are in good agreement with the experimental data. In Table 1 we report the formation enthalpies of the optimized geometries of the eight possible transition states (TSs) that originate from the 2–7' intramolecular  $\text{S}_{\text{E}}\text{Ar}$  reaction of **B** and the analogous 6–7'  $\text{S}_{\text{E}}\text{Ar}$  reaction of **B'** (Figure 3a and 3b). Of course, in these transition states all *E/Z* geometries get lost. Only two among the eight calculated TSs show a marked stability, namely 6–7'-*ct* (*cis-trans* referring to the relative positions of 6-H, 7'-H and 8'-H), leading to compounds (±)-7/(±)-16 with 7'–8' *trans* fusion, and 2–7'-*ct* (*cis-trans* referring to the relative positions of 2-H, 7'-H and 8'-H), affording the intermediate **C'**, which evolves to the benzo[*k*]xanthene products **6/15**. The optimized geometries of the most stable TSs for the proposed  $\text{S}_{\text{E}}\text{Ar}$  mechanism are reported in Figure 4.

Table 1.  $\Delta H_{\text{f}}$  and Boltzmann distribution for the optimized geometries of the eight possible transition states (TSs) originating from the 6–7' and 2–7' intramolecular  $\text{S}_{\text{E}}\text{Ar}$  reaction of **B**.

TS	$\Delta H_{\text{f}}$ [kcal mol <sup>-1</sup> ]	Boltzmann distribution [%]
6–7'- <i>ct</i>	–202.97	36.54
6–7'- <i>tc</i>	–200.42	0.51
6–7'- <i>tt</i>	–200.31	0.42
6–7'- <i>cc</i>	–198.97	0.04
2–7'- <i>ct</i>	–203.29	62.40
2–7'- <i>tc</i>	–199.03	0.05
2–7'- <i>tt</i>	–198.98	0.05
2–7'- <i>cc</i>	–188.13	0.00



Scheme 3. Mechanism for the formation of compounds **6** and **15**.

Figure 3. a) 6–7' and b) 2–7' intramolecular  $S_EAr$  reactions.Figure 4. Optimized geometries of the most stable transition states for the proposed  $S_EAr$  mechanism.

The relative percentages from the Boltzmann populations of the more stable TS (62.40% for **2-7'-ct** and 36.54% for **6-7'-ct**) are quite in agreement with the higher yields observed for the benzo[*k*]xanthene lignans **6** and **15**. Note here also that the **6-7'-ct** TS, by far the most stable among those leading to aryldihydronaphthalenes, produces the stereoisomers ( $\pm$ )-**7** and ( $\pm$ )-**16** with *trans* stereochemistry of the substituents at C-1 and C-2. This result is in perfect agreement with all the literature data on the syntheses of aryldihydronaphthalene lignans by oxidative coupling, which invariably report the diastereomer with *trans* substitution as the main product.<sup>[22]</sup>

The observation that dihydrobenzofuran neolignan analogues of compounds **3** and **4** were not obtained, at least as the main products, in the  $MnO_2$ -mediated coupling reactions with both caffeic esters **1** and **5** prompted us to carry out the coupling reaction in the presence of  $Ag_2O$ , which is frequently reported in the literature as the oxidative agent in the dimerization of phenylpropanoids.<sup>[24]</sup>

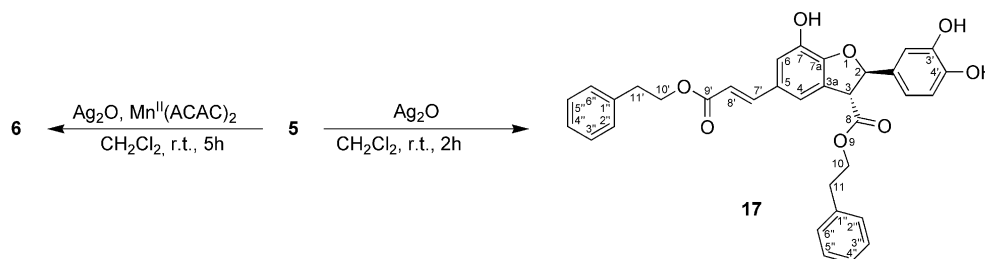
It was immediately apparent that the treatment of **5** with  $Ag_2O$  in  $CH_2Cl_2$  at room temperature gives rise to a more complex reaction mixture. A study of the dependence of the conversion rate and yield on the time and oxidant/substrate molar ratio (see Exp. Sect.) showed that with a molar ratio of 1:2, the main product, different to **6**, is formed after 90 min (yield 58%; conversion 68%).

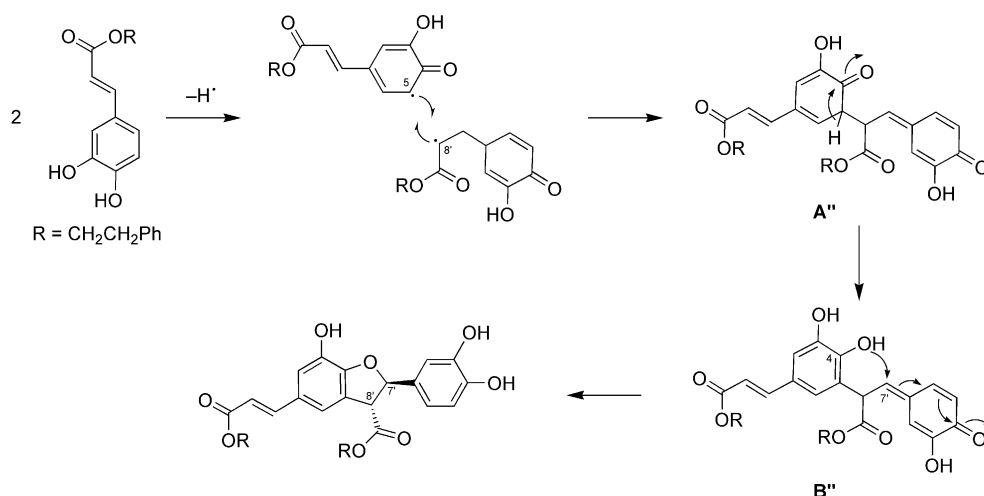
Preparative coupling allowed the isolation and characterization of this product as the dihydrobenzofuran neolignan ( $\pm$ )-**17** [Scheme 4; only the (2*R*,3*R*) enantiomer is reported], obtained as a racemate. The spectroscopic data for ( $\pm$ )-**17** are in agreement with those of related dihydrobenzofuran neolignans previously reported in the literature.<sup>[25]</sup> The expected *trans* stereochemistry of the substituents at C-2 and C-3 was established on the basis of the  $J_{1,2}$  value (7.0 Hz).<sup>[25]</sup>

The result of the  $Ag_2O$ -mediated coupling reaction clearly indicates that the oxidative agent may play a major role in directing the formation of either the dihydrobenzofuran neolignans or the benzoxanthene lignans, yielding <1% products in the presence of  $Ag_2O$ . To establish whether the  $MnO_2$ -mediated reaction could be influenced by the presence of  $Mn^{2+}$  ions formed by the reduction of  $MnO_2$ , we carried out the coupling reaction of **5** with  $Ag_2O$  in the presence of  $Mn(ACAC)_2$ . Under these conditions, a 54% conversion of CAPE was observed and the main product was again the benzoxanthene lignan **6** (51%). The aryldihydronaphthalene lignan ( $\pm$ )-**7** was detected in trace amounts, whereas the neolignan ( $\pm$ )-**17** was undetectable (Scheme 4).

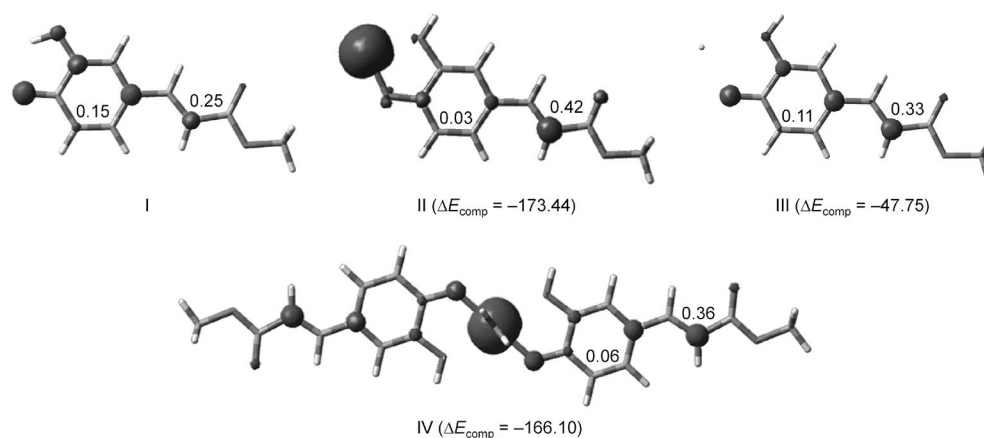
These data strongly suggest that  $Mn^{2+}$  ions can stabilize radicals derived from caffeic esters by complexation of the *o*-hydroxyquinone form, which favours 8–8' coupling instead of 5–8' coupling. The latter leads to dihydrobenzofuran neolignans, according to a previously reported mechanism,<sup>[18a]</sup> as detailed in Scheme 5.

To corroborate this hypothesis, we performed a DFT computational study by utilizing methyl caffeate as the model compound starting from its most stable conformation.<sup>[26]</sup> Methyl caffeate radicalization yields the 3-OH and

Scheme 4. Oxidative coupling of compound **5** with  $Ag_2O$  and  $Ag_2O/Mn^{II}(ACAC)_2$ .



Scheme 5. Mechanism for the formation of compounds (±)-17.

Figure 5. Optimized geometries and spin density distributions for the methyl caffeate radical and its complexes with  $\text{Ag}^+$  and  $\text{Mn}^{2+}$ .  $\Delta E$  in  $\text{kcal mol}^{-1}$ .

4-OH radicals, the latter being the more stable (about  $2.37 \text{ kcal mol}^{-1}$ ) due to the more extended electronic delocalization in the presence of the *p*- $\text{CH}=\text{CHCO}_2\text{Me}$  group.

Accordingly, complexes of the methyl caffeate radical at the 4-position with both  $\text{Mn}^{2+}$  and  $\text{Ag}^+$  were optimized and the spin density distributions of these radical cations are reported in Figure 5 together with that of the parent caffeate radical. The values of  $\Delta E$  for complex formation are also reported. In the case of the manganese complexes, the high-spin complex is more stable than the low-spin one.

Figure 5 clearly shows for the  $\text{Mn}^{\text{II}}$  complex **II** a dramatic variation of the spin density at C-5 (0.03) and C-8 (0.42) in comparison with the uncomplexed radical **I** (0.15 and 0.25, respectively): the spin density at C-5 is reduced to almost zero whereas at C-8 it is strongly enhanced. This implies a tendency towards 8–8' coupling. Conversely, in the  $\text{Ag}^{\text{I}}$  complex **III**, the densities at C-5 (0.11) and C-8 (0.33) are not significantly changed and, in principle, a mixture of 5–5', 5–8' and 8–8' coupling could occur. The formation of one main product by 5–8' coupling can be explained on the basis of other arguments.

Then, taking into account the fact that the activation energies for the radical coupling reactions are nearly zero,<sup>[27]</sup> we compared the stability of all the possible diastereomeric products arising from the 5–5', 5–8' and 8–8' coupling reactions of the methyl caffeate 4-OH radical to establish the expected percentage distribution. A preliminary Monte Carlo<sup>[28]</sup>-simulated annealing<sup>[29]</sup> was used to sample geometries from a Boltzmann-weighted distribution. The heating time was set to 10000 steps followed by a constant temperature simulation, that is, 400 K, with  $1 \times 10^5$  steps and finally a cooling time of  $2 \times 10^4$  steps. The geometries obtained were selected within a range of  $10.0 \text{ kcal mol}^{-1}$  in terms of the energy difference between the isomers and in the next step a full optimization of the selected geometries was carried out by using the semiempirical AM1 Hamiltonian. The lowest  $\Delta H_f$  values obtained for each series are reported in Table 2. On the basis of these results, and considering the sum of each diastereoisomeric pair derived from the same type of coupling, the 5–5' coupling should be the predominant process, furnishing 64.65% of the adduct, followed by the 5–8' reaction with a yield of 31.87%

and only traces of the 8–8' coupling (3.48%). Nevertheless, in the case of the 5–5' coupling of Ag<sup>+</sup>-complexed caffeate radicals the two molecules are constrained to approach each other in a head-to-head fashion, and it is reasonable that the repulsion between the two positively charged regions could preclude the incoming reaction, thus causing the formation, through 5–8' coupling, of the dihydrobenzofuran neolignan as the largely predominant product.

Table 2.  $\Delta H_f$  and Boltzmann distribution for all the possible diastereomeric products arising from 5–5', 5–8' and 8–8' coupling reactions of the methyl caffeate radical.

Coupling product	$\Delta H_f$ [kcal mol <sup>-1</sup> ]	Boltzmann distribution [%]
5–5'-( <i>R,R</i> )	–231.709	60.41
5–5'-( <i>R,S</i> )	–230.125	4.24
5–8'-( <i>R,R</i> )	–231.104	21.90
5–8'-( <i>R,S</i> )	–230.635	9.97
8–8'-( <i>R,R</i> )	–229.557	1.63
8–8'-( <i>R,S</i> )	–229.631	1.85

Finally, we tried to obtain a higher CAPE conversion and a better yield of the unusual benzo[*k*]xanthene lignan **6**. First, we tested various solvent systems. In Table 3 we report the results of this screening. Although toluene allowed a higher conversion of CAPE, the highest yield of **6** (72%) was obtained in chloroform. The more oxygenated solvents gave both low conversion and low yield of the main

product **6**. The highest yield of the minor product **7** (23.7%) was obtained with an *n*-hexane/dichloromethane (1:1) mixture.

In the attempt to improve the conversion rate, we examined a further Mn-based oxidative agent, namely Mn(OAc)<sub>3</sub>. We studied the conversion and yield with respect to the substrate. The oxidative agent ratio showed that the benzoxanthene lignan **6** is obtained in 71% yield and 89% conversion in 6 h (CHCl<sub>3</sub>, room temperature) with a 1:4 CAPE/Mn(OAc)<sub>3</sub> ratio (Table 4). Under these conditions the minor product **7** was obtained in 22% yield. Thus, this appears the most convenient way to obtain **6**, with the further advantage of the simple use of the reagent and an easier work-up of the reaction mixture.

We applied this methodology to the synthesis of the natural benzoxanthene lignans mongolicumin A (**10**) and rufescidride (**9**). First, we tried to obtain mongolicumin A by direct oxidative coupling of caffeic acid in various solvent systems, but the reaction was unsatisfactory due to the formation of a complex mixture with low yields (<10%) of the benzo[*k*]xanthene product. Thus we turned to a different strategy (Scheme 6). In the first step, the benzo[*k*]xanthene lignan **15** was subjected to alkaline hydrolysis to give **18**. By subsequent cyclization under acidic conditions, this afforded rufescidride (**9**). A mild basic hydrolysis of **9** allowed mongolicumin A (**10**) to be obtained in a good overall yield (40% from caffeic acid).

Table 3. Conversions and yields of **6** and **7** in various solvent systems.<sup>[a]</sup>

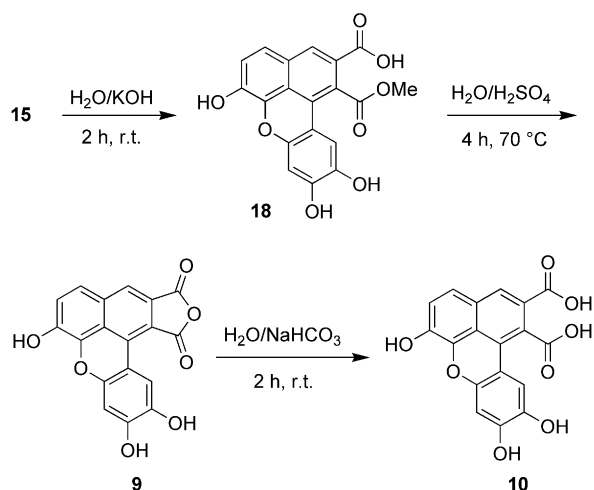
Entry	Solvent	Conversion [%] <sup>[b]</sup>	Yield [%] of <b>6</b> <sup>[c]</sup>	Yield [%] of (±)- <b>7</b> <sup>[d]</sup>
1	CHCl <sub>3</sub>	67 ± 2	72 ± 2	2.8 ± 0.3
2	<i>n</i> -hexane/CH <sub>2</sub> Cl <sub>2</sub> (1:1)	79 ± 2	57 ± 3	23.7 ± 2.1
3	CCl <sub>4</sub>	82 ± 5	55 ± 6	21.8 ± 2.4
4	toluene	92 ± 3	53 ± 5	3.2 ± 0.6
5	CH <sub>2</sub> Cl <sub>2</sub>	68 ± 1	48 ± 4	16.5 ± 0.9
6	<i>t</i> BuOH	25 ± 7	20 ± 5	3.6 ± 0.7
7	Et <sub>2</sub> O	38 ± 6	11 ± 1	3.3 ± 0.6
8	dioxane	34 ± 4	10 ± 1	nd <sup>[e]</sup>
9	EtOAc	45 ± 6	7 ± 2	1.5 ± 0.3
10	MeOH	39 ± 2	7 ± 3	1.2 ± 0.2
11	THF	42 ± 2	4 ± 1	n.d. <sup>[e]</sup>
12	MeCN	45 ± 4	4 ± 3	n.d. <sup>[e]</sup>
13	Me <sub>2</sub> (CO)	32 ± 1	2 ± 1	n.d. <sup>[e]</sup>

[a] Reactions were performed at 298 K on the 7 mm scale using a 1:3.2 oxidant (MnO<sub>2</sub>)/substrate ratio. The data were determined by HPLC analysis (in triplicate) of the crude reaction mixture. [b] The data are referenced to **5** as the standard. [c] The data are referenced to **6** as the standard. [d] The data are referenced to **7** as the standard. [e] n.d.: not detected.

Table 4. Conversion and yield with respect to the substrate/oxidant ratio.<sup>[a]</sup>

Entry	Substrate/oxidant	Conversion [%] <sup>[b]</sup>	Yield [%] of <b>6</b> <sup>[c]</sup>	Yield [%] of (±)- <b>7</b> <sup>[d]</sup>
1	1:0.5	56 ± 3	30.6 ± 2	20.0 ± 2
2	1:1	61 ± 6	33.8 ± 2	23.3 ± 2
3	1:2	72 ± 7	57.4 ± 3	28.9 ± 1
4	1:3	83 ± 6	63.5 ± 3	26.5 ± 4
5	1:4	89 ± 4	70.9 ± 4	21.9 ± 3
6	1:8	97 ± 4	48.1 ± 2	8.3 ± 1

[a] Reactions were performed in CHCl<sub>3</sub> at 298 K using Mn(OAc)<sub>3</sub> as the oxidative agent. The data were determined by HPLC analysis (in triplicate) of the crude reaction mixture. [b] The data are referenced to **5** as the standard. [c] The data are referenced to **6** as the standard. [d] The data are referenced to **7** as the standard.



Scheme 6. Synthesis of compounds 18, 9 and 10.

## Conclusions

The phenolic oxidative coupling reactions of CAPE (caffeic acid phenethyl ester, **5**) and methyl caffeate (**1**) have been carried out under various conditions. Among them Mn(OAc)<sub>3</sub> in CHCl<sub>3</sub> afforded the new benzo[*k*]xanthene lignans **6** and **15** in good yields and allowed the synthesis of the natural lignans mongolicumin A (**10**) and rufescidride (**9**). Further, the previously unreported racemic *trans*-dihydronaphthalene lignans (±)-**7** and (±)-**16** were obtained from Mn-mediated caffeic ester dimerization. In the presence of Ag<sub>2</sub>O the main product was the previously unreported racemic *trans*-dihydrobenzofuran neolignan (±)-**17**. A mechanism for the formation of these dimers has been proposed and corroborated by experimental data and calculations. Note here that an “orientation” effect towards 8–8′ coupling was observed in the presence of MnO<sub>2</sub> and Mn(OAc)<sub>3</sub>.

In contrast to aryldihydronaphthalene lignans, benzo[*k*]xanthene lignans are rarely encountered in nature. To the best of our knowledge, this is the second reported synthesis of a benzo[*k*]xanthene lignan by oxidative coupling and the first one to be synthesized in considerable yield. A further point worth noting is that the benzo[*k*]xanthene lignan yunnanic acid H (**11**) and the aryldihydronaphthalene lignan radosiin (**14**), both dimers of rosmarinic acid and structurally related to compounds **6** and (±)-**7**, respectively, have previously been isolated by the same plant, *Salvia yunnanensis*.<sup>[16]</sup> This is a strong indication of the biomimetic nature of the synthesis reported herein and supports the hypothesis that the natural products **10** and **14** are formed in nature through a mechanism very similar to that proposed here. The “unnatural” lignans **6** and (±)-**7** are closely related to known natural products and, in principle, may be “natural” products biogenetically related to CAPE and not yet discovered in nature.

The biomedical importance of the aryldihydronaphthalene lignans and dihydrobenzofuran neolignans has already been cited above. In particular, radosiin (**14**) is an

antioxidant, antiallergic<sup>[30]</sup> and an inhibitor of Type I DNA topoisomerase.<sup>[31]</sup> The dihydrobenzofuran (±)-**17** is related to bioactive neolignans such as compounds **2–4**. Of these, **3** has been very recently reported as a promising cell death inducer by modulating the mitochondrial pathway and G2/M cell cycle arrest.<sup>[4]</sup> The benzoxanthenes **6** and **15** are related to compounds reported as potential antitumour agents.<sup>[32]</sup> In addition, the benzoxanthene lignans are strongly fluorescent both in solution and in the solid state under UV light at 366 nm (Figure 6), and this property may be of considerable interest in the design of new fluorescent probes for biomedical applications.<sup>[33]</sup> In conclusion, we think that these biomimetic syntheses will be useful for the future exploitation and study of the above cited lignans and neolignans or their analogues.

Figure 6. A reversed round-bottomed flask containing a solid sample of the benzo[*k*]xanthene lignan **6**, photographed under UV light (366 nm).

## Experimental Section

**General:** NMR spectra were recorded with a Varian Unity Inova spectrometer operating at 499.86 (1H) and 125.70 MHz (13C) and equipped with a gradient-enhanced, reverse-detection probe. Chemical shifts ( $\delta$ ) are referenced to TMS solvent signals. All NMR experiments, including two-dimensional spectra, that is, COSY, HSQC, HMBC and NOEDS, were performed by using software supplied by the manufacturers and acquired at constant temperature (298 K). UV/Vis spectra were recorded using a Perkin–Elmer Lambda 25 spectrophotometer. The fluorescence spectrum was recorded with a Spex Fluorolog-2 (mod. F-111) spectrofluorimeter; the fluorescence quantum yield was obtained by using anthracene in CH<sub>2</sub>Cl<sub>2</sub> as the standard ( $\Phi_F = 0.27$ ). IR spectra were recorded with a Perkin–Elmer Spectrum BX FT-IR System spectrometer. High-performance liquid chromatography (HPLC) was carried out using an Agilent Series G1354A pump and an Agilent UV G1314A detector. An auto-sampler Agilent Series 1100 G1313A was used for sample injection.



The qualitative and quantitative analyses of the reaction mixtures were carried out by HPLC–UV using a reversed-phase column (Luna® C18 column, 5 µm; 4.6 × 250 mm; Phenomenex) and the following solvent system: eluent A: H<sub>2</sub>O; eluent B: CH<sub>3</sub>CN. The elution gradient had the following profile:  $t_{0\text{min}} = 100\%$  A,  $t_{40\text{min}} = 100\%$  B,  $t_{50\text{min}} = 100\%$  B; the flow rate was 1 mL min<sup>-1</sup>. The chiral HPLC analyses of the racemates [(±)-7], (±)-16 and (±)-17 were carried out by HPLC–UV using a Chiralpak® IA column (5 µm; 4.6 × 250 mm). Liquid chromatography–mass spectrometry (LC–ESI-MS) was carried out with an HPLC Waters 1525 instrument equipped with a Waters Micromass ZQ2000 mass spectrometer. LiChroprep Si-60 and LiChroprep DIOL 25–40 (Merck) were used as stationary phases for column chromatography. TLC was carried out by using precoated silica gel F<sub>254</sub> plates (Merck). Cerium sulfate and phosphomolybdic acid were used as spray reagents. All chemicals except MnO<sub>2</sub> were of reagent grade and used as purchased from Sigma–Aldrich. MnO<sub>2</sub> was prepared as described previously.<sup>[34]</sup> Elemental analyses were performed with a Perkin–Elmer 240B microanalyser.

**Theoretical Approach:** Semiempirical and quantum mechanical calculations were carried out at the AM1<sup>[35]</sup> and DFT<sup>[36]</sup> levels of theory, respectively, in the gas phase. For DFT calculations the B3LYP functional was employed which combines the three-coefficient-dependent hybrid functional for the exchange energy proposed by Becke (B3)<sup>[37]</sup> with the correlation functional proposed by Lee, Yang and Parr (LYP).<sup>[38]</sup> Pople's 6-311G(d) basis set was used for all elements except silver and manganese, for which the effective core potential LANL2DZ was used.<sup>[39]</sup> Moreover, the unrestricted open-shell approach in conjunction with the 6-311G(d) basis set was used for radical species, allowing the best results to be obtained both with regard to calculation time and correlation with experimental data in the study of aroxyl radicals.<sup>[40]</sup> The doublet nature of the radicals was confirmed by the values of the  $S^2$  operator. Before annihilation of the first spin contaminant, the  $S^2$  values were found to be about 0.75 in all cases. The spin densities for each atom were obtained by summing the diagonal terms of the spin density matrix. For manganese complexes both high- and low-spin states were considered. All calculations were carried out with the Gaussian03 suite of programs.<sup>[41]</sup> For each molecule studied, a full geometry optimization was performed with no constraints and the harmonic vibrational frequencies were calculated at the same level of theory with the aim to characterize all structures as minima or saddle points. For the minima, all the wavenumbers obtained were positive, whereas in the case of the transition states (TSs) only one wavenumber was imaginary. This unique imaginary frequency, which is associated with the transition vector,<sup>[42]</sup> describes the atomic motion at the TS and can be used to trace the intrinsic reaction coordinate<sup>[43]</sup> (IRC analysis) pathway that connects the reactants and products.

**Reaction of CAPE with MnO<sub>2</sub>:** A solution of CAPE (100 mg, 0.35 mmol) in CH<sub>2</sub>Cl<sub>2</sub> (25 mL) was added to a stirred suspension of MnO<sub>2</sub> (300 mg, 3.5 mmol) in CH<sub>2</sub>Cl<sub>2</sub> (25 mL). The reaction mixture was then stirred at room temperature for 4 h and treated with a saturated solution of ascorbic acid in methanol. After filtration, the solvent was removed under reduced pressure and the yellow-brown residue obtained was purified by column chromatography over silica gel using a gradient of CH<sub>2</sub>Cl<sub>2</sub>/MeOH (from 0 to 4%) to provide **6** (42 mg, 42.7%) and **7** (12 mg, 12.1%).

**Bis(2-phenylethyl) 6,9,10-Trihydroxybenzo[*k*]xanthene-1,2-dicarboxylate (6):** Yellow amorphous powder.  $R_f$  (TLC) = 0.36 (8% MeOH/CH<sub>2</sub>Cl<sub>2</sub>). UV (CH<sub>2</sub>Cl<sub>2</sub>):  $\lambda_{\text{max}}$  ( $\epsilon$ ) = 271 (27700), 386 (11000 M<sup>-1</sup> cm<sup>-1</sup>) nm. IR (CHCl<sub>3</sub>):  $\tilde{\nu}$  = 3522, 3346, 2952, 2925, 2852,

1716, 1599, 1453, 1192, 1144, 1086 cm<sup>-1</sup>. <sup>1</sup>H NMR [500 MHz, (CD<sub>3</sub>)<sub>2</sub>CO, 298 K]:  $\delta$  = 8.08 (s, 1 H, 3-H), 7.47 [d,  $^3J_{\text{H,H}}$  = 8.5 Hz, 1 H, 4-H], 7.4–7.2 (m, 10 H, 2''''-H, 3''''-H, 4''''-H, 5''''-H, 6''''-H), 7.36 (overlapped with other signals, 1 H, 5-H), 7.28 (overlapped with other signals, 1 H, 11-H), 6.72 (s, 1 H, 8-H), 4.62 (t,  $^3J_{\text{H,H}}$  = 9.0 Hz, 2 H, 1''-H), 4.47 (t,  $^3J_{\text{H,H}}$  = 9.0 Hz, 2 H, 1''-H), 3.10 (t,  $^3J_{\text{H,H}}$  = 7.0 Hz, 2 H, 2''-H, 2''-H) ppm. <sup>13</sup>C NMR [125 MHz, (CD<sub>3</sub>)<sub>2</sub>CO, 298 K]:  $\delta$  = 170.8 (2'-CO), 166.7 (3'-CO), 149.0 (C-7a), 148.3 (C-9), 142.6 (C-6), 142.1 (C-10), 138.9 (C-1''''), 137.5 (C-6a), 129.8 (C-2''''), C-6''''), 129.6 (C-3), 129.2 (C-3''''), C-5''''), 127.5 (C-3a), 127.4 (C-4''''), 126.3 (C-11b), 125.1 (C-2), 123.9 (C-11c), 122.6 (C-1), 122.1 (C-4), 120.6 (C-5), 110.6 (C-11a), 112.1 (C-11), 104.4 (C-8), 66.6 (C-1'', C-1'''), 35.7 (C-2''), 34.9 (C-2''') ppm. For selected COSY, NOESY and HMBC correlations see Figure 1. MS (ESI):  $m/z$  = 561 [M – H]<sup>-</sup>. C<sub>34</sub>H<sub>26</sub>O<sub>8</sub>: calcd. C 72.59, H 4.66; found C 72.23, H 4.68.

**Bis(2-phenylethyl) 1-(3,4-Dihydroxyphenyl)-6,7-dihydroxy-1,2-dihydro-naphthalene-2,3-dicarboxylate [(±)-7]:** Yellow-brown amorphous powder.  $R_f$  (TLC) = 0.21 (8% MeOH/CH<sub>2</sub>Cl<sub>2</sub>). UV (EtOH):  $\lambda_{\text{max}}$  ( $\epsilon$ ) = 248 (15100), 330 (8620 M<sup>-1</sup> cm<sup>-1</sup>), nm. IR (CHCl<sub>3</sub>):  $\tilde{\nu}$  = 3524, 2920, 1702, 1603, 1512, 1453, 1262, 1190 cm<sup>-1</sup>. <sup>1</sup>H NMR [500 MHz, (CD<sub>3</sub>)<sub>2</sub>CO, 298 K]:  $\delta$  = 7.55 (s, 1 H, 4-H), 7.19–7.30 (m, 10 H, aromatic rings), 6.94 (s, 1 H, 5-H), 6.69 (d,  $^3J_{\text{H,H}}$  = 8.5 Hz, 2 H, 5'-H), 6.59 (s, 1 H, 8-H), 6.45 (d,  $^4J_{\text{H,H}}$  = 1.5 Hz, 1 H, 2'-H), 6.40 (dd,  $^3J_{\text{H,H}}$  = 8.5,  $^4J_{\text{H,H}}$  = 1.5 Hz, 1 H, 6'-H), 4.36 (d,  $^3J_{\text{H,H}}$  = 2.5 Hz, 1 H, 1-H), 4.28 (m, 2 H, 1''-H)\*, 4.19 (m, 2 H, 1''-H)\*, 3.86 (d,  $^3J_{\text{H,H}}$  = 2.5 Hz, 1 H, 2-H), 2.94 (t,  $^3J_{\text{H,H}}$  = 7.0 Hz, 2 H, 2''-H)#, 2.83 (t,  $^3J_{\text{H,H}}$  = 7.0 Hz, 2 H, 2''-H)# ppm. <sup>13</sup>C NMR [125 MHz, (CD<sub>3</sub>)<sub>2</sub>CO, 298 K]:  $\delta$  = 172.5 (3-CO<sub>2</sub>R)<sup>§</sup>, 166.9 (2-CO<sub>2</sub>R)<sup>§</sup>, 147.9 (C-6), 145.4 (C-7), 144.8 (C-4'), 144.4 (C-3'), 138.9 (C-1''), 138.3 (C-4), 136.1 (C-1'), 130.7 (C-8a), 129.7 (C-2''''), C-6''''), 129.1 (C-3''''), C-5''''), 127.0 (C-4''''), 124.7 (C-4a), 122.9 (C-3), 119.5 (C-5), 116.9 (C-8), 116.6 (C-6'), 115.8 (C-5'), 115.2 (C-2'), 65.9 (C-1''')\*, 65.6 (C-1''')\*, 48.3 (C-2), 46.0 (C-1), 35.6 (C-2''')#, 35.5 (C-2''')# ppm. Values with identical superscripts may be interchanged. MS (ESI):  $m/z$  = 565.4 [M – H]<sup>-</sup>. C<sub>34</sub>H<sub>30</sub>O<sub>8</sub>: calcd. C72.07, H 5.34; found C 72.01, H 5.28. For NOESY and COSY correlations see Figure 2. Chiral HPLC analysis at 330 nm: Chiralpak® IA (5 µm; 4.6 × 250 mm), 2-propanol/hexane (30:60), flow rate of 0.5 mL min<sup>-1</sup>, retention time: 26.31, 30.45 min.

**Acetylation of 6:** Compound **6** (20 mg, 0.035 mmol) was dissolved in pyridine (2 mL) and acetic anhydride (2 mL). The solution was stirred at room temperature for 3 h and, after standard work-up, the peracetate **8** was obtained in 95% yield.

**Bis(2-phenylethyl) 6,9,10-Tris(acetyloxy)benzo[*k*]xanthene-1,2-dicarboxylate (8):** Yellow amorphous powder.  $R_f$  (TLC) = 0.18 (100% CH<sub>2</sub>Cl<sub>2</sub>). UV (CH<sub>2</sub>Cl<sub>2</sub>):  $\lambda_{\text{max}}$  ( $\epsilon$ ) = 258 (18254), 376 (7689 M<sup>-1</sup> cm<sup>-1</sup>) nm. IR (CHCl<sub>3</sub>):  $\tilde{\nu}$  = 2914, 1770, 1724, 1587, 1413, 1257, 1172, 1016 cm<sup>-1</sup>. <sup>1</sup>H NMR [500 MHz, (CD<sub>3</sub>)<sub>2</sub>CO, 298 K]:  $\delta$  = 8.36 (s, 1 H, 3-H), 7.71 (d,  $^3J_{\text{H,H}}$  = 8.5 Hz, 1 H, 5-H), 7.53 (d,  $^3J_{\text{H,H}}$  = 8.5 Hz, 1 H, 4-H), 7.39–7.20 (m, 10 H, aromatic rings), 4.58 (t,  $^3J_{\text{H,H}}$  = 7.5 Hz, 2 H, 1''-H), 4.51 (t,  $^3J_{\text{H,H}}$  = 7.5 Hz, 2 H, 2''-H), 3.12 (t,  $^3J_{\text{H,H}}$  = 7.0 Hz, 2 H, 2'-H), 3.09 (t,  $^3J_{\text{H,H}}$  = 7.0 Hz, 2 H, 1'-H), 2.41, 2.33 and 2.31 (each s, 3 H, COCH<sub>3</sub>) ppm. <sup>13</sup>C NMR [125 MHz, (CD<sub>3</sub>)<sub>2</sub>CO, 298 K]:  $\delta$  = 172.8, 169.7, 168.1, 167.8, 167.3, 165.1, 149.7, 143.5, 141.2, 138.1, 137.4, 134.9, 134.2, 130.8, 130.1, 128.8, 128.7, 128.4, 128.2, 127.2, 126.5, 126.3, 124.8, 124.3, 123.6, 123.4, 121.3, 120.2, 116.7, 112.4, 66.7, 65.9, 34.8, 34.1, 26.2, 22.5 ppm. MS (ESI):  $m/z$  = 687 [M – H]<sup>-</sup>.

**Synthesis of Methyl Caffeate (1):** Conc. H<sub>2</sub>SO<sub>4</sub> (2 mL) was added to a solution of caffeic acid (1 g, 5.5 mmol) in MeOH (70 mL). The resulting mixture was stirred for 1 h at reflux. After cooling at room

temp., ethyl acetate (200 mL) was added to the mixture. The organic phase was washed with a NaHCO<sub>3</sub> solution and saturated brine, dried with anhydrous Na<sub>2</sub>SO<sub>4</sub> and the solvent evaporated under vacuum to yield **1** (yield 99%). The <sup>1</sup>H NMR spectroscopic data for the product are in perfect agreement with literature data.<sup>[44]</sup>

**Reaction of Methyl Caffate with MnO<sub>2</sub>:** A solution of methyl caffate (75 mg, 0.36 mmol) in CH<sub>2</sub>Cl<sub>2</sub> (25 mL) was added to a stirred suspension of MnO<sub>2</sub> (300 mg, 3.5 mmol) in CH<sub>2</sub>Cl<sub>2</sub> (25 mL). The reaction mixture was then stirred at room temperature for 4 h and then treated with a saturated solution of ascorbic acid in methanol. After filtration, the solvent was removed under reduced pressure and the yellow-brown residue obtained was purified by column chromatography over silica gel using a gradient of CH<sub>2</sub>Cl<sub>2</sub>/MeOH (from 0 to 4%) to give **15** (37 mg, 51%) and (±)-**16** (5 mg, 7%).

**Dimethyl 6,9,10-Trihydroxybenzo[k]xanthene-1,2-dicarboxylate (15):** Yellow amorphous powder. *R<sub>f</sub>* (TLC) = 0.57 (8% MeOH/CH<sub>2</sub>Cl<sub>2</sub>). UV (MeOH): λ<sub>max</sub> (ε) = 270 (24254), 393 (11051 M<sup>-1</sup> cm<sup>-1</sup>) nm. IR (Nujol): ν̄ = 3288, 2715, 1712, 1674, 1598, 1461, 1377, 1274, 1153, 1087 cm<sup>-1</sup>. <sup>1</sup>H NMR [500 MHz, (CD<sub>3</sub>)<sub>2</sub>CO, 298 K]: δ = 8.17 (s, 1 H, 3-H), 7.53 (d, <sup>3</sup>J<sub>H,H</sub> = 8.5 Hz, 1 H, 4-H), 7.33 (d, <sup>3</sup>J<sub>H,H</sub> = 8.5 Hz, 1 H, 5-H), 7.19 (s, 1 H, 11-H), 6.72 (s, 1 H, 8-H), 3.97 (s, 3 H, OCH<sub>3</sub>), 3.88 (s, 3 H, OCH<sub>3</sub>) ppm. <sup>13</sup>C NMR [125 MHz, (CD<sub>3</sub>)<sub>2</sub>CO, 298 K]: δ = 171.2 (2-CO), 166.9 (1-CO), 149.0 (C-7a), 147.7 (C-9), 142.7 (C-6), 142.5 (C-10), 137.5 (C-6a), 129.6 (C-3), 127.4 (C-3a), 125.6 (C-11b), 124.9 (C-2), 124.1 (C-11c), 122.1 (C-4), 121.6 (C-2), 120.6 (C-5), 110.7 (C-11a), 112.5 (C-11), 104.6 (C-8), 52.8 and 52.5 (OCH<sub>3</sub>) ppm. MS (ESI): *m/z* = 381 [M - H]<sup>-</sup>. C<sub>20</sub>H<sub>14</sub>O<sub>8</sub>: calcd. C 62.83, H 3.69; found C 62.75, H 3.72.

**Dimethyl 1-(3,4-Dihydroxyphenyl)-6,7-dihydroxy-1,2-dihydronaphthalene-2,3-dicarboxylate [(±)-16]:** Yellow amorphous powder. *R<sub>f</sub>* (TLC) = 0.47 (8% MeOH/CH<sub>2</sub>Cl<sub>2</sub>). IR, UV, MS and NMR spectroscopic data are in agreement with literature data.<sup>[19]</sup> Chiral HPLC analysis at 250 nm: Chiralpak® IA (5 μm; 4.6 × 250 mm), 2-propanol/hexane (30:60), flow rate of 0.5 mL min<sup>-1</sup>, retention time: 12.61, 25.26 min.

**Reaction of CAPE with Ag<sub>2</sub>O:** A solution of CAPE (200 mg, 0.704 mmol) in CHCl<sub>3</sub> (10 mL) was added to a stirred suspension of Ag<sub>2</sub>O (163 mg, 0.703 mmol) in CHCl<sub>3</sub> (10 mL). The reaction mixture was then stirred at room temperature for 2 h. After filtration, the solvent was removed under reduced pressure and the dark-brown residue obtained was purified by column chromatography over silica gel using a gradient of CH<sub>2</sub>Cl<sub>2</sub>/MeOH (from 0 to 8%) to provide (±)-**17** (35 mg, 17.6%).

**2-Phenylethyl 2-(3,4-Dihydroxyphenyl)-7-hydroxy-5-[(1E)-3-oxo-3-(2-phenylethoxy)prop-1-enyl]-2,3-dihydro-1-benzofuran-3-carboxylate [(±)-17]:** Yellow-brown amorphous powder. *R<sub>f</sub>* (TLC) = 0.55 (8% MeOH/CH<sub>2</sub>Cl<sub>2</sub>). UV (MeOH): λ<sub>max</sub> (ε) = 330 (17705 M<sup>-1</sup> cm<sup>-1</sup>) nm. IR (CHCl<sub>3</sub>): ν̄ = 3536, 3030, 2955, 1733, 1702, 1619, 1607, 1496, 1263, 1170, 1135 cm<sup>-1</sup>. <sup>1</sup>H NMR [500 MHz, (CD<sub>3</sub>)<sub>2</sub>CO, 298 K]: δ = 8.20 (br. s, 2 H, 3-OH, 4-OH), 7.52 (d, <sup>3</sup>J<sub>H,H</sub> = 16.0 Hz, 7'-H), 7.35–7.20 (m, 10 H, aromatic rings), 7.14 (d, <sup>3</sup>J<sub>H,H</sub> = 1.5 Hz, 1 H, 6-H), 6.92 (d, <sup>3</sup>J<sub>H,H</sub> = 1.5 Hz, 1 H, 4-H), 6.89 (d, <sup>4</sup>J<sub>H,H</sub> = 2.0 Hz, 1 H, 2'-H), 6.87 (d, <sup>3</sup>J<sub>H,H</sub> = 8.0 Hz, 1 H, 5'-H), 6.76 (dd, <sup>3</sup>J<sub>H,H</sub> = 8.0, <sup>4</sup>J<sub>H,H</sub> = 2.0 Hz, 1 H, 6'-H), 6.26 (d, <sup>3</sup>J<sub>H,H</sub> = 16.0 Hz, 8'-H), 5.95 (d, <sup>3</sup>J<sub>H,H</sub> = 7.0 Hz, 2-H), 4.46 (t, <sup>3</sup>J<sub>H,H</sub> = 7.0 Hz, 2 H, 10'-H), 4.41 (t, <sup>3</sup>J<sub>H,H</sub> = 7.0 Hz, 2 H, 10-H), 4.31 (d, <sup>3</sup>J<sub>H,H</sub> = 7.0 Hz, 3-H), 3.03 (t, <sup>3</sup>J<sub>H,H</sub> = 7.0 Hz, 4 H, 11-H, 11'-H) ppm. <sup>13</sup>C NMR [125 MHz, (CD<sub>3</sub>)<sub>2</sub>CO, 298 K]: δ = 171.0 (C-8), 167.1 (C-9'), 149.9 (C-7), 146.3 (C-4'), 146.1 (C-3'), 145.4 (C-7'), 142.4 (C-7a), 139.2 (C-1''), 138.9 (C-1'''), 132.6 (C-1'), 129.7 (C-2''), C-6''), 129.68 (C-5), 129.6 (C-2''', C-6'''), 129.2 (C-3'', C-

5''), 129.1 (C-3''', C-5'''), 127.3 (C-5'), 127.1 (C-4'''), 118.6 (C-6'), 117.8 (C-4), 117.0 (C-5), 116.1 (C-5'), 116.0 (C-8'), 113.8 (C-2'), 87.8 (C-2), 66.6 (C-10'), 65.3 (C-10''), 56.3 (C-3), 35.7 (C-7'''), 35.4 (C-7''') ppm. MS (ESI): *m/z* = 589 [M + Na]<sup>+</sup>. C<sub>34</sub>H<sub>30</sub>O<sub>8</sub>: calcd. C 72.07, H 5.34; found C 75.25, H 5.30. Chiral HPLC analysis at 330 nm: Chiralpak® IA (5 μm; 4.6 × 250 mm), ethanol/hexane (80:20), flow rate of 0.6 mL min<sup>-1</sup>, retention time: 8.86, 10.96 min.

**Reaction of CAPE with Ag<sub>2</sub>O in the Presence of Mn(ACAC)<sub>2</sub>:** A solution of CAPE (4 mg, 0.014 mmol) in CHCl<sub>3</sub> (10 mL) was added to a stirred suspension of Ag<sub>2</sub>O (13 mg, 0.056 mmol) and Mn(ACAC)<sub>2</sub> (14 mg, 0.140 mmol) in CHCl<sub>3</sub> (2 mL). The reaction mixture was then stirred at room temperature for 5 h. Then, a saturated solution of ascorbic acid in MeOH was added. The solvent was evaporated under vacuum to yield a residue which was analysed by HPLC.

**Reactions of CAPE with Mn(OAc)<sub>3</sub>:** Mn(OAc)<sub>3</sub> (substrate/oxidative agent ratio 1:0.5, 1:1, 1:2, 1:3, 1:4, 1:8) was added to six aliquots (2 mL) of a solution of CAPE (40 mg, 0.07 mmol) dissolved in CHCl<sub>3</sub> (20 mL). For each aliquot the reaction was replicated three times. The reaction mixtures were stirred for 6 h at room temperature (the reactions were monitored at regular time intervals by TLC). Then a saturated solution of ascorbic acid in MeOH was added. After filtration the solvent was evaporated in vacuo and the residue was dissolved in MeOH (10 mL)/H<sub>2</sub>O (200 mL). Subsequently the mixture was extracted twice with EtOAc. The organic phase, after washing with a solution of NaHCO<sub>3</sub> and saturated brine, was dried with anhydrous Na<sub>2</sub>SO<sub>4</sub> and the solvent evaporated under vacuum to yield a residue which was analysed by HPLC. The results are reported in Table 4.

**Reaction of Caffeic Acid with Mn(OAc)<sub>3</sub>:** Mn(OAc)<sub>3</sub> (23 mg, 0.086 mmol, substrate/oxidative agent ratio 1:4) was added to nine stirred aliquots of caffeic acid (4 mg, 0.021 mmol) in chloroform (2 mL), acetone or ethyl acetate (for each solvent the reaction was replicated three times). The reaction mixtures were stirred for 8 h at room temperature, after which the solvent was removed in vacuo and a saturated solution of ascorbic acid in MeOH (2 mL) was added to all samples. The filtrate solutions were analysed by HPLC. The averages and standard deviations of the caffeic acid conversions and mongolicumin A (**10**) yields are as follows: chloroform: conversion 48 ± 5%, yield 3 ± 2%; acetone: conversion 93 ± 3%, yield 6 ± 2%; ethyl acetate: conversion 74 ± 5%, yield 9 ± 3%.

**Synthesis of 18:** Compound **15** (50 mg, 0.13 mmol) was dissolved under nitrogen in 2 M aqueous potassium hydroxide (10 mL). The solution was stirred for 2 h at room temperature. Then the solution was acidified with 2 N HCl and extracted with ethyl acetate, the organic layer was washed with water and saturated brine and dried with Na<sub>2</sub>SO<sub>4</sub>. The solvent was removed under reduced pressure to obtain **18** (48 mg, 99%) as a brown powder. *R<sub>f</sub>* (TLC-RP<sub>18</sub>) = 0.18 (50% MeOH/H<sub>2</sub>O). UV (MeOH): λ<sub>max</sub> (ε) = 263 (18100), 392 (6301 M<sup>-1</sup> cm<sup>-1</sup>) nm. IR (Nujol): ν̄ = 3468, 3389, 1707, 1681, 1258, 1190 cm<sup>-1</sup>. <sup>1</sup>H NMR (500 MHz, CD<sub>3</sub>OD, 298 K): δ = 8.14 (s, 1 H, 3-H), 7.38 (d, <sup>3</sup>J<sub>H,H</sub> = 8.5 Hz, 1 H, 4-H), 7.23 (d, <sup>3</sup>J<sub>H,H</sub> = 8.5 Hz, 1 H, 5-H), 7.09 (s, 1 H, 11-H), 6.70 (s, 1 H, 8-H), 4.02 (s, 3 H, OCH<sub>3</sub>) ppm. <sup>13</sup>C NMR (125 MHz, CD<sub>3</sub>OD, 298 K): δ = 172.3, 168.0, 148.2, 146.9, 141.6, 141.5, 136.9, 128.8, 128.6, 126.2, 125.2, 123.2, 124.2, 121.3, 120.2, 111.6, 109.7, 103.9, 51.8 ppm. Selected NOESY correlation: 4.02 and 7.09. MS (ESI): *m/z* = 367 [M - H]<sup>-</sup>. C<sub>19</sub>H<sub>12</sub>O<sub>8</sub>: calcd. C 61.96, H 3.28; found C 61.75, H 3.32.

**Synthesis of Rufescidride (9):** Compound **18** (33 mg, 0.09 mmol) was dissolved in 2 M sulfuric acid solution (50 mL) and warmed at 70 °C for 4 h. The aqueous phase was extracted with ethyl acetate

(4 × 50 mL) and then the organic layer was washed with water and saturated brine and dried with Na<sub>2</sub>SO<sub>4</sub>. The solvent was removed under reduced pressure to give **9** (30 mg) as a red powder in quantitative yield. The ESI-MS spectrum and NMR spectroscopic data are in perfect agreement with literature data.<sup>[45]</sup>

**Synthesis of Mongolicumin A (10):** Compound **9** (23 mg, 0.06 mmol) was dissolved in ethyl acetate (50 mL) and added under nitrogen to an aqueous solution of 2 M sodium hydrogen carbonate (100 mL). The solution was vigorously stirred for 2 h. Then the organic layer, containing **10**, after standard work-up, was recuperated and furnished **9** (5 mg, conversion 80%). The aqueous phase was acidified with 2 M HCl until pH ≈ 2 and extracted with ethyl acetate (3 × 100 mL). The organic layer was washed with a solution of NaHCO<sub>3</sub> and saturated brine and dried with Na<sub>2</sub>SO<sub>4</sub>. The solvent was removed under reduced pressure to give **10** (18 mg, 95%) as a yellow-brown powder. The ESI-MS spectrum and NMR spectroscopic data are in perfect agreement with literature data.<sup>[46]</sup>

## Acknowledgments

This research was supported by a grant from the Università degli Studi di Catania (Progetti di Ricerca di Ateneo, Catania, Italy) and by Ministero dell'Università e della Ricerca (MIUR) (PRIN 2007, Rome, Italy). The authors acknowledge Prof. Salvatore Sortino (Università degli Studi di Catania) for determination of the fluorescence data. CPU time from the Italian supercomputing center CI-NECA is also acknowledged.

- [1] R. D. Haworth, *J. Chem. Soc.* **1942**, 448–456.
- [2] a) G. P. Moss, *Pure Appl. Chem.* **2000**, *72*, 1493–1523; b) <http://www.chem.qmul.ac.uk/iupac/lignan/>.
- [3] D. R. Gang, A. T. Dinkova-Kostova, L. B. Davin, N. G. Lewis, *Phylogenetic links in plant defense systems: lignans, isoflavonoids, and their reductases*, in: *Phytochemicals for Pest Control*, ACS Symposium Series, **1997**, vol. 658, pp. 58–89.
- [4] J. S. Bose, V. Gangan, R. Prakash, S. K. Jain, S. K. Manna, *J. Med. Chem.* **2009**, *52*, 3184–3190.
- [5] a) S. Apers, A. Vlietinck, L. Pieters, *Phytochem. Rev.* **2004**, *2*, 201–207; b) S. Van Miert, S. Van Dyck, T. J. Schmidt, R. Brun, A. Vlietinck, G. Lemiere, L. Pieters, *Bioorg. Med. Chem.* **2005**, *13*, 661–669; c) A. K. Prasad, V. Kumar, P. Arya, S. Kumar, R. Dabur, N. Singh, A. K. Chhillar, G. L. Sharma, B. Ghosh, J. Wengel, C. E. Olsen, V. S. Parmar, *Pure Appl. Chem.* **2005**, *77*, 25–40.
- [6] S. Apers, D. Paper, J. Buergermeister, S. Baronikova, S. Van Dyck, G. Lemiere, A. Vlietinck, L. Pieters, *J. Nat. Prod.* **2002**, *65*, 718–720.
- [7] E. L. Ghisalberti, *Phytomedicine* **1997**, *4*, 151–166.
- [8] J. L. Charlton, *J. Nat. Prod.* **1998**, *61*, 1447–1451.
- [9] L. B. Davin, H.-B. Wang, A. L. Crowell, D. L. Bedgar, D. M. Martin, S. Sarkanen, N. G. Lewis, *Science* **1997**, *275*, 362–366.
- [10] L. Pieters, S. Van Dyck, M. Gao, R. Bai, E. Hamel, A. Vlietinck, G. Lemiere, *J. Med. Chem.* **1999**, *42*, 5475–5481.
- [11] a) R. Kerbel, J. Folkman, *Nat. Rev. Cancer* **2002**, *2*, 727–739; b) Y. Crawford, N. Ferrara, *Cell Tissue Res.* **2009**, *335*, 261–269.
- [12] a) V. Cardile, L. Lombardo, C. Spatafora, C. Tringali, *Bioorg. Chem.* **2005**, *33*, 22–33; b) S. Grasso, L. Siracusa, C. Spatafora, M. Renis, C. Tringali, *Bioorg. Chem.* **2007**, *35*, 137–152.
- [13] a) F. M. Da Cunha, D. Duma, J. Assreuy, F. C. Buzzi, R. Niero, M. M. Campos, J. B. Calixto, *Free Radical Res.* **2004**, *38*, 1241–1253; b) Y.-T. Lee, M.-J. Don, P.-S. Hung, Y.-C. Shen, Y.-S. Lo, K.-W. Chang, C.-F. Chen, L.-K. Ho, *Cancer Lett.* **2005**, *223*, 19–25; c) X. Debing, W. Dong, H. Yujun, X. Jiayin, Z. Zhaoyang, L. Zengpeng, X. Jiang, *Anti-Cancer Drugs* **2006**, *17*, 753–762; d) H. H. Jin, P. H. Joo, C. Hwa-Jin, M. Hye-Young, P. Eun-Jung, H. Ji-Young, L. S. Kook, *J. Nutr. Biochem.* **2006**, *17*, 356–362.
- [14] C. Spatafora, C. Tringali, *Targets in Heterocyclic Systems. Chemistry and Properties*, **2007**, vol. 11, pp. 284–312.
- [15] S. A. Souza da Silva, A. L. Souto, M. de Fatima Agra, E. V. Leitao da-Cunha, J. M. Barbosa-Filho, M. Sobral da Silva, R. Braz-Filho, *ARKIVOC* **2004**, *6*, 54–58.
- [16] S. Shi, Y. Zhang, K. Huang, S. Liu, Y. Zhao, *Food Chem.* **2008**, *108*, 402–406.
- [17] T. Tanaka, A. Nishimura, Y. Kouno, G. Nonaka, C.-R. Yang, *Chem. Pharm. Bull.* **1997**, *45*, 1596–1600.
- [18] a) S. Maeda, H. Masuda, T. Tokoroyama, *Chem. Pharm. Bull.* **1994**, *42*, 2506–2513; b) S. Maeda, H. Masuda, T. Tokoroyama, *Chem. Pharm. Bull.* **1995**, *43*, 935–940.
- [19] I. Agata, T. Hatano, S. Nishibe, T. Okuda, *Chem. Pharm. Bull.* **1988**, *36*, 3223–3225.
- [20] I. Agata, T. Hatano, S. Nishibe, T. Okuda, *Phytochemistry* **1989**, *28*, 2447–2450.
- [21] R. S. Ward, *Chem. Soc. Rev.* **1982**, *11*, 75–125.
- [22] M. Orlandi, B. Rindone, G. Molteni, P. Rummakko, G. Brunow, *Tetrahedron* **2001**, *57*, 371–378.
- [23] A. Pelter, R. S. Ward, R. R. Rao, *Tetrahedron* **1985**, *41*, 2933–2938.
- [24] a) M. Bruschi, M. Orlandi, B. Rindone, P. Rummakko, L. Zoia, *J. Phys. Org. Chem.* **2006**, *19*, 592–596; b) G. Lemièrre, M. Gao, A. De Groot, R. Dommissie, J. Lepoivre, L. Pieters, V. Buss, *J. Chem. Soc. Perkin Trans. 1* **1995**, 1775–1779.
- [25] S. M. O. Van Dyck, G. L. F. Lemièrre, T. H. M. Jonckers, R. Dommissie, *Molecules* **2000**, *5*, 153–161.
- [26] N. F. L. Moncado, R. Calheiros, S. M. Fiuza, F. Borges, A. Gaspar, J. Garrido, M. P. Marques, *J. Mol. Model.* **2007**, *13*, 865–877.
- [27] C. J. Houtman, *Holzforchung* **1999**, *53*, 585–589.
- [28] N. Metropolis, A. W. Rosenbluth, M. N. Rosenbluth, A. N. Teller, E. Teller, *J. Chem. Phys.* **1953**, *21*, 1087–1092.
- [29] S. Kirkpatrick, C. D. Gelatt, M. P. Vecchi, *Science* **1983**, *220*, 671–680.
- [30] H. Ito, T. Miyazaki, M. Ono, H. Sakurai, *Bioorg. Med. Chem.* **1998**, *6*, 1051–1056.
- [31] Y. Kashiwada, K. F. Bastow, K.-H. Lee, *Bioorg. Med. Chem. Lett.* **1995**, *5*, 905–908.
- [32] N. C. Birnberg, Q. Weng, H. Liu, J. Avruch, J. Kyriakis, PCT Int. Appl. **2004**, 36 pages; [*Chem. Abstr.* **2004**, *141*, 1222–1258].
- [33] L. Patsenker, A. Tatars, O. Kolosova, O. Obukhova, Y. Povrozin, I. Fedyunyayeva, I. Yermolenko, E. Terpetschnig, *Ann. N. Y. Acad. Sci.* **2008**, *1130*, 179–187.
- [34] C. Daquino, M. C. Foti, *Tetrahedron* **2006**, *62*, 1536–1547.
- [35] a) M. J. S. Dewar, E. G. Zoebisch, E. F. Healy, J. J. P. Stewart, *J. Am. Chem. Soc.* **1985**, *107*, 3902–3909; b) M. J. S. Dewar, C. Jie, J. Yu, *Tetrahedron* **1993**, *49*, 5003–5038.
- [36] P. Hohenberg, W. Kohn, *Phys. Rev. B* **1964**, *136*, 864–871.
- [37] a) A. D. Becke, *Phys. Rev. A* **1988**, *38*, 3098–3100; b) A. D. Becke, *J. Chem. Phys.* **1993**, *98*, 5648–5652.
- [38] C. Lee, W. Yang, R. G. Parr, *Phys. Rev. B* **1988**, *37*, 785–789.
- [39] P. J. Hay, W. R. Wadt, *J. Chem. Phys.* **1985**, *82*, 270–283; P. J. Hay, W. R. Wadt, *J. Chem. Phys.* **1985**, *82*, 284–298; P. J. Hay, W. R. Wadt, *J. Chem. Phys.* **1985**, *82*, 299–310.
- [40] W. Bors, C. Michel, K. Stettmaier, S. P. Kazazić, L. Klasinc, *Croat. Chem. Acta* **2002**, *75*, 957–964.
- [41] M. J. Frisch, G. W. Trucks, H. B. Schlegel, G. E. Scuseria, M. A. Robb, J. R. Cheeseman, V. G. Zakrzewski, J. A. Montgomery Jr., R. E. Stratmann, J. C. Burant, S. Dapprich, J. M. Millam, A. D. Daniels, K. N. Kudin, M. C. Strain, O. Farkas, J. Tomasi, V. Barone, M. Cossi, R. Cammi, B. Mennucci, C. Pomelli, C. Adamo, S. Clifford, J. Ochterski, G. A. Petersson, P. Y. Ayala, Q. Cui, K. Morokuma, D. K. Malick, A. D. Rabuck, K. Raghavachari, J. B. Foresman, J. Cioslowski, J. V. Ortiz, B. B. Stefanov, G. Liu, A. Liashenko, P. Piskorz, I. Komaromi, R. Gomperts, R. L. Martin, D. J. Fox, T. Keith, M. A. Al-Laham, C. Y. Peng, A. Nanayakkara, C. Gonzalez, M.

- Challacombe, P. M. W. Gill, B. Johnson, W. Chen, M. W. Wong, J. L. Andres, C. Gonzalez, M. Head-Gordon, E. S. Replogle, J. A. Pople, *Gaussian03, Revision D.02*, Gaussian, Inc., Wallingford, CT, **2004**.
- [42] J. W. Mciver Jr., *Acc. Chem. Res.* **1974**, *7*, 72–77.
- [43] a) K. Fukui, *Acc. Chem. Res.* **1981**, *14*, 363–368; b) M. Head-Gordon, J. A. Pople, *J. Chem. Phys.* **1988**, *89*, 5777–5786.
- [44] M. C. Foti, C. Daquino, C. Geraci, *J. Org. Chem.* **2004**, *69*, 2309–2314.
- [45] S. A. Souza da Silva, A. Lopes Souto, M. de Fátima Agra, E. V. Leitão da-Cunha, J. M. Barbosa-Filho, M. Sobral da Silva, R. Braz-Filhoc, *ARKIVOC* **2004**, *6*, 54–58.
- [46] S. Shi, Y. Zhao, H. Zhou, Y. Zhang, X. Jiang, K. Huang, *J. Chrom. A* **2008**, *1209*, 145–152.

Received: July 17, 2009

Published Online: November 6, 2009